

Diseños óptimos para modelos compartimentales biocinéticos

* *López Fidalgo J.¹, Rodríguez Díaz J.M.¹, Sánchez León G.², Santos Martín M.T.¹*

¹fidalgo@usal.es, juanmrod@usal.es, maysam@usal.es, Departamento de Estadística, Universidad de Salamanca

²guillerm@usal.es, Departamento de Economía y Empresa, Universidad de Salamanca

*Alphabetic order

Resumen

The flow of radioactive particles inside the body from internally deposited radioisotopes in people exposed to inhalation, ingestion, injection or other ways is usually evaluated using compartmental models (see Sánchez and López-Fidalgo 2003 and López-Fidalgo and Sánchez 2004). ICRP 66 describes the model of the human respiratory tract, represented by two main regions. One of these, the thoracic region (lungs) is divided into different compartments. The retention in lungs is given for a large combination of ratios of exponential sums depending on time. In this paper, a large two-parameter model is studied and a simplified model is proposed. The local c-optimal designs for the main parameters are obtained using the results of López-Fidalgo and Rodríguez-Díaz (2003). The initial model is reduced in order to obtain optimal designs in a more suitable way. Efficiencies for all the computed designs are provided in compared.

Keywords: Biokinetic model, compartmental model, optimal design, radioactivity retention.

AMS: 62K05

1. Introduction

Compartmental models are used to analyze a system by dividing it into a finite number of components, which are called compartments. The compartments interact each other exchanging different products, e.g. chemical substances, hormones, people from a population, etc. A compartmental model is a network where the nodes are compartments connected by arrows designing the flow of some substance from one to another. In particular, the flow and retention of some kind of “substance” will be considered. There are initial compartments where the intake (input) of the substance takes place and there are also final compartments from where the substance is eliminated (output). A general introduction to this theory can be found in Anderson (1983).

Let be a general compartmental model with compartments denoted by numbers, $i = 1, 2, 3, \dots, n + 1$. This model will include the flow corresponding to the disintegrating rate of each compartment. Let $k_{i,j}$ be the rate of transfer from compartment i to compartment j . For simplicity k_i will be used instead of $k_{i,j}$ if there is not possible confusion. Let $q_i(t)$ be the retention in compartment i at time t and $b_i(t)$ the input coming from the environment to compartment i at time t . The content at compartment i can be represented by the equations:

$$\frac{\partial q_i(t)}{\partial t} = \sum_r k_{r,i} q_r(t) - \sum_j k_{i,j} q_i(t) + b_i(t) = \sum_r k_{r,i} q_r(t) - k_i q_i(t) + b_i(t). \quad (1)$$

If possible, a system will be decomposed in catenary unidirectional chains. A catenary unidirectional system is a sequence of compartments in such a way that each one receives flow from the previous one, with rate k_i , and it gives flow to the next one, with rate k_{i+1} . The first one receives flow from the environment, $b_1(t)$, and only the last one gives flow to the environment, with rate k_n . Disintegrating rates, $k_{i,0}$, $i = 1, 2, \dots, n$, for each compartment will be considered as well. Figure 1 shows this situation. Then, where it has been said flow to the environment it would be said flow to the environment or other compartments outside the chain.

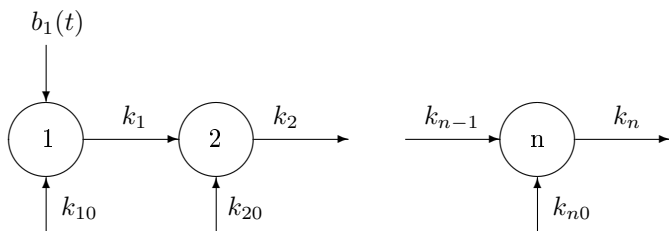


Figure 1: Catenary unidirectional system with n compartments

If the rates of transfer, K_i , in a unidirectional catenary system are all different an explicit solution for the retention is derived straightforward for the case of an impulse (acute) input b_1 at time $t = 0$ (Skrable et al 1974),

$$q_i(t) = b_1 \left(\prod_{p=1}^{i-1} k_p \right) \sum_{j=0}^i \left(\frac{e^{-K_j t}}{\prod_{p=0, p \neq j}^i (K_p - K_j)} \right) e^{-\lambda_k t}, \quad i = 1, 2, \dots, n \quad (2)$$

where λ_R is the radioactive decay constant of isotope. If there is not radioactive isotope then $\lambda_R = 0$.

Thus, it would be very convenient to decompose a system in catenary unidirectional chains, if possible.

Compartmental systems are usually described by using flow diagrams, and are widely used in medicine, chemistry pharmacokinetics,... In fact, the human body is usually seen and studied as an example of a compartmental model, divided into several regions. We are interested in one of them, the respiratory tract.

ICRP 66 describes the compartmental model of the human respiratory tract applied to the intake of radioactive aerosols by inhalation. The respiratory tract is represented by five regions. The extrathoracic airways are divided in a *nasal passage* and a *posterior nasal and oral passages* (the pharynx and the larynx), and finally the thoracic region is divided into *bronchial*, *bronchiolar* and *alveolar-interstitial*.

In this paper, the case of an instantaneous (acute) intake of a radioactive substance in the human body will be considered. The model we deal with meters the pulmonary retention of this substance along the time t (in days). The compartmental system for the thoracic tract will be solved in the next section. Thus, it will be possible to get the retention in lungs, which would be given by a large combination of fractions of sums of exponential terms depending on time.

2. Solving the respiratory tract model

The previous ideas have been applied to solve the respiratory tract model (ICRP 66) applied to the intake of radioactive aerosols by inhalation (Figure ??).

In the ICRP 66 model the material from environment is deposited in the respiratory tract in compartments labeled "Particles in Initial State" (PIS), except in the lymphatic nodes (represented by compartment 10 and 13), and in ET_1 . From each PIS compartment the material is transferred into the body fluids, at an absorption rate s_p . It is also simultaneously transferred from PIS (at a rate s_{pt}) to a corresponding compartment labeled "Particles in Transformed State" (PTS). The flow goes from 1 (in PIS) to 1 (in PTS), from 2 (in PIS) to 2 (in PTS), and so on. We can consider that each compartment 1,...,13 in PIS has a mirror compartment 1,...,13 in PTS. In each compartment in PTS the isotope is dissolved at a constant rate s_p into the body fluids (usually the blood). For instance, the total transfer rate for AI_2 in PIS will be $K_{AI_2} = k_{2,4} + s_{pt} + s_p$, and for AI_2 in PTS will be $K'_{AI_2} = k_{2,4} + s_t$. This general model of RT is common to any element. The absorption rates $\{s_{pt}, s_p, s_t\}$ are related with the chemical form of the element. ICRP 66 establishes three types of materials according to its absorption behavior: fast (F), moderate (M), and slow (S).

We are interested in evaluating the retention in lungs for an acute intake I_0 at time $t = 0$. Lungs are represented by compartments 1 to 10 in PIS and their “mirror” compartments 1 to 10 in PTS. This region can be divided in catenary branches (more than 50). Each catenary branch starts in the deposition compartments, that is in compartments 1 to 9 in PIS. The fractions deposited in these compartments are called the Initial Deposition Factors, $IDF = IDF_1, \dots, IDF_9$. They are functions of the Activity Median Aerodynamic Diameter (AMAD), later represented by p , physiological factors of the subject, as well as various condition of exposure. IDF can be calculated following the procedure described in ICRP 66 or obtained from Annex F of ICRP 66.

ICRP 66 already gives the deposition factor values for IDF_{AI} , $IDF_{bbfast+seq}$, IDF_{bbslow} , $IDF_{BBfast+seq}$, IDF_{BBslow} , where $IDF_{AI} = IDF_1 + IDF_2 + IDF_3$, $IDF_{bbfast+seq} = IDF_4 + IDF_6$, $IDF_{bbslow} = IDF_5$, $IDF_{BBfast+seq} = IDF_7 + IDF_9$, $IDF_{BBslow} = IDF_8$.

ICRP 66 also provides the following relationships: $IDF_1 = 0.3IDF_{AI}$, $IDF_2 = 0.6$, IDF_{AI} , $IDF_3 = 0.1IDF_{AI}$, $IDF_{bb} = IDF_{bbfast+seq} + IDF_{bbslow}$, $IDF_6 = 0.007IDF_{bb}$, $IDF_{BB} = IDF_{BBfast+seq} + IDF_{BBslow}$, $IDF_9 = 0.007IDF_{BB}$. This means that we can derive the $\{IDF_1, \dots, IDF_9\}$ values using the values of IDF_{AI} , $IDF_{bbfast+seq}$, IDF_{bbslow} , $IDF_{BBfast+seq}$, IDF_{BBslow} .

Now, we can use equation (1) to compute the content in all compartments of the thoracic region (lungs) for a worker exposed to aerosols particles type S . For type S the absorption rates values, in $d-1$, are $spt = 0.1$, $sp = 100$, $st = 0.0001$. The solution of equation (2) is represented in Figure 3 for this case. It shall taken into account that $b_1 = I \times IFD_i$. The solution (Sánchez 2004) obtained as a function of IDF_{AI} , $IDF_{bbfast+seq}$, IDF_{bbslow} , $IDF_{BBfast+seq}$, IDF_{BBslow} and t is represented in Figure 2. IDF_{AI} , $IDF_{bbfast+seq}$, IDF_{bbslow} , $IDF_{BBfast+seq}$, IDF_{BBslow} are function of p (AMAD). The procedure described in ICRP 66 for obtaining these values involved long algebraic expressions. However we have found that the IFD parameters, in the range of interest of AMAD $[0.5\mu m, 20\mu m]$ may fitted using the following equations:

$$\begin{aligned}
 IDF_{AI}(p) &= 0.128187e^0.170111 \\
 IDF_{bbfast+seq}(p) &= 0.0100737e^0.0878945 \\
 IDF_{bbslow}(p) &= 0.0212844e^4.35327 + 0.00920991e^0.147244 \\
 IDF_{BBfast+seq}(p) &= 0.0171738e^0.566783 + 0.0171738e^0.0577835 \\
 IDF_{BBslow}(p) &= 0.0110839e^1.11147 + 0.0110839e^1.23578
 \end{aligned} \tag{3}$$

These parameters can be replaced in the equation given in Figure 2 obtaining the retention as a rational function of p and t . This model, $E[y(t)] =$

$\eta(t, I, p)$, $t \in [0, T]$ is rather complex to deal with. The parameters are the initial intake I and the particles' size p . The model is linear in I but not in p . The bigger the particles are, the more easily they are eliminated. Furthermore, the retention at time 0 is not I but a fraction of I . This is because we pay attention only to lung's retention, while I is the global intake in the whole body.

Usually I is between 500 and 1500 Bq, and p varies between 1 and 10 units. Figure 3 represents the initial model for $I=1000$, $p=5$.

3. Optimal designs for the original model

Let us assume there is only one worker. First let us consider the case when two observations y_{t_1} , y_{t_2} are taken from the worker at times t_1 and t_2 respectively. These are repeated measurements and need to be considered in the optimal design theory in a particular way taking into account the existing correlation between the observations. For a recent reference on these kind of problem see Müller and Stehlík (2004). For the case considered here the following result comes easily.

Proposition: Neither the D -optimal design depends on the linear parameter I nor the c -optimal designs do for $c = c_1 = (1, 0)^t$ or $c = c_2 = (0, 1)^t$.

Proof: The model can be written as

$$\nabla\eta(t, I, p) = I f_1(t, p).$$

Denoting $f_2(t, p) = \partial f_1(t, p)/\partial p$ the linearized model then

$$\begin{aligned} \nabla\eta(t, I, p) &= \left(\frac{\partial\eta(t, I, p)}{\partial I}, \frac{\partial\eta(t, I, p)}{\partial p} \right)^t \\ &= (f_1(t, p), I f_2(t, p))^t = B(I) (f_1(t, p), f_2(t, p))^t, \end{aligned}$$

with

$$B = B(I) = \begin{pmatrix} 1 & 0 \\ 0 & I \end{pmatrix}.$$

The information matrix is

$$M = X^t \Sigma X = B \tilde{X}^t \Sigma \tilde{X} B = B \tilde{M} B,$$

where Σ is the covariance matrix,

$$\tilde{X} = \begin{pmatrix} f_1(t_1, p) & f_2(t_1, p) \\ f_1(t_2, p) & f_2(t_2, p) \end{pmatrix} \text{ and } \tilde{M} = \tilde{X}^t \Sigma \tilde{X},$$

that does not depend on I .

The proof finish taking into account that

$$\text{Det}(M) = \text{Det}(B)^2 \text{Det}(\tilde{M}), \quad \text{and} \quad \Phi_c(M) = c^t M^{-1} c = \Phi_{B^{-1}c}(\tilde{M}).$$

□

Let us now consider

$$\Sigma = \sigma^2 \begin{pmatrix} 1 & e^{-\rho d} \\ e^{-\rho d} & 1 \end{pmatrix},$$

where the covariance between the two samples t_1 y t_2 depends on the distance $d = t_2 - t_1$.

We will show the optimal designs for different criterion functions and several values for ρ . We consider also two different design intervals. The linearized model will be used, so that taking into account the previous result we can restrict the model to $(f_1(t, p), f_2(t, p))^t$, not depending on I . The initial value for p will be set to $p = 5$.

3.1. Interval $[0, T]$

Previous and posterior results lead us to fix the first observation at the very first possible moment. In theory, this moment is $t = 0$. Table 1 shows the optimal times to take the second sample depending on the value of ρ and the different optimization criteria.

ρ	D	ϕ_{c_1}	ϕ_{c_2}
0.001	0.14741	0.08762	0.05502
0.01	0.20447	0.12837	0.09834
0.1	0.20695	0.14016	0.14242
1	0.23138	0.15572	0.16778
10	2.19645	2.94087	2.81104
100	2.19645	2.94087	2.81103
1000	2.19645	2.94087	2.81103

Table 1: Second observation's time for different values of ρ when the first observation is fixed at $t = 0$ (Original Model)

3.2. Interval $[0.5, T]$

Actually the practitioner needs some time to start taking observations. This period must be at least 12 hours in our case, what moves the design

interval to $[0.5, T]$. Again, when fixing the first observation at the beginning of the interval the second is shown in Table 2 for different values of ρ and for several optimality criteria.

ρ	D	ϕ_{c_1}	ϕ_{c_2}
0.001	1.15473	1.01307	0.96813
0.01	1.15284	1.09390	1.09354
0.1	1.16246	1.13000	1.13699
1	69.0073	88.8826	88.0903
10	69.0198	88.8826	88.0903
100	69.0198	88.8826	88.0903
1000	69.0198	88.8826	88.0903

Table 2: Second observation's time for different ρ , first observation fixed at time $t = 0.5$ (Original Model)

Remark:

It is easy to see that the smaller is ρ , the closer must be the two samples. In other words, when there is a strong relationship between observations the best design chooses them very close to each other.

Furthermore, there are big differences in choosing the best day to take the second observation for the two starting points $t = 0$ and $t = 0.5$. The explanation for the different results is that the model's curvature is specially concentrated in the interval $[0,1]$. This fact is specially clear in the geometric computation of the c -optimal designs using Elfving's method (1952) (see Figures 4 and 5). The last one shows one of Elfving's set branches, increasing t in 0.5 units each time. It can be seen that for $t > 1$ the plot is almost a straight line.

4. Reduced model

If we pay attention to the original model we can see that all the denominators of the fractions do not depend on t , what lead us to the theoretical model:

$$Approx(I, t, p) = I \frac{\gamma_1 e^{\alpha_1 p + \beta_1 t} + \gamma_2 e^{\alpha_2 p + \beta_2 t}}{1 + \gamma_3 e^{\alpha_3 p}}.$$

We will focus on D -optimization. Let us take

$$x = e^t, \quad \theta = e^p.$$

The linearized model can be reduced to

$$(f_1(x, \theta), f_2(x, \theta))^t,$$

with

$$f_1(x, \theta) = \frac{\gamma_1 \theta^{\alpha_1} x^{\beta_1} + \gamma_2 \theta^{\alpha_2} x^{\beta_2}}{1 + \gamma_3 \theta^{\alpha_3}}; \quad f_2(x, \theta) = \frac{\partial f_1(x, \theta)}{\partial \theta}.$$

In the homoscedastic case, with uncorrelated observations, the determinant of the information matrix can be written as

$$\det(M) = g(\sigma, \gamma, \alpha, \tilde{\alpha}, \beta) (x^{\beta_1} - x^{\beta_2})^2,$$

$\gamma = (\gamma_1, \gamma_2, \gamma_3)^t$, $\tilde{\alpha} = (\alpha_1, \alpha_2, \alpha_3)^t$, $\beta = (\beta_1, \beta_2)^t$, where g is a function not depending on x . The value for x maximizing the determinant will always be the upper limit of the design interval, except for $\beta_1 < 0$ and $\beta_2 < 0$, which gives the point

$$x^* = \left(\frac{b1}{b2} \right)^{\frac{1}{b1-b2}},$$

with $b1 = -\beta_1$, $b2 = -\beta_2$. That means

$$t^* = \frac{\ln b_1 - \ln b_2}{b_1 - b_2} \quad \text{or} \quad y^* = \left(\frac{b1}{b2} \right),$$

when choosing the mapping $y = e^{-t(\beta_1 - \beta_2)}$.

On the other hand, we can assume now the covariance matrix

$$\Sigma = \sigma^2 e^t p^2 \begin{pmatrix} 1 & e^{-\alpha t} \\ e^{-\alpha t} & 1 \end{pmatrix},$$

that takes into account that the variance increases with t and p . The latter is due to the fact that the bigger the particles are, the more easily are eliminated, having smaller values for the retention, and making the measure instruments not so accurate. Now, using the mappings we have seen before, the determinant of the information matrix can be written as

$$\det(M) = g(\sigma, \gamma, \alpha, \tilde{\alpha}, \beta) \frac{x^{-2(1-\alpha)} (x^{\beta_1} - x^{\beta_2})^2}{x^{2\alpha} - 1},$$

$\gamma = (\gamma_1, \gamma_2, \gamma_3)^t$, $\tilde{\alpha} = (\alpha_1, \alpha_2, \alpha_3)^t$, $\beta = (\beta_1, \beta_2)^t$, with g independent of x . When t is large, $x^{2\alpha} = e^{2t\alpha} \gg 1$, and the determinant can be approached by $(x^{\beta_1-1} - x^{\beta_2-1})^2$, giving

$$x^* = \left(\frac{b1+1}{b2+1} \right)^{\frac{1}{b1-b2}}.$$

5. Discussion

Figure 6 shows the determinant of the original model (linearized for $p = 5$) in terms of the first point t_1 and the distance $d = t_2 - t_1$. In the first graph (top to the left) t_1 is taken to be between 0 and 2 and d varying between 0 and 100. For a fixed d the function seems to be decreasing in t_1 , and that is the reason why t_1 must be fixed to be the first point of the design interval. It can be seen that the optimal value for d is close (but different) to 0 (top to the right graph). This behaviour changes after a while, for greater values of t_1 . The function starts to increase with d a second time after this local maximum near 0. Furthermore, the valley structure is gradually reduced and eventually vanishes (bottom to the left graph). Finally, after this “second” increasing the function decreases again for the rest of the values of d (bottom to the right graph).

This is the explanation of the “jump” that can be observed when computing the optimal value for $d = t_2 - t_1$ as a function of t_1 . At the beginning, the maximum of the determinant is attained for small values of d , the top of the first “hill”. As t_1 increases this first hill gets flatter, and at some point the second one turns out to be the maximum value. Thus, the “jump” appears when the maximum moves from the first hill to the second one as t_1 increases.

6. Bibliography

- [1] Anderson D.H. (1983). *Compartmental modeling and tracer kinetics*. Lecture notes in biomathematics 50; Springer-Verlag: Berlin.
- [2] Elfving G. (1952). Optimum allocation in linear regression theory. *Ann. Statist.*, **23**, 255-262.
- [3] López-Fidalgo, J. and Sánchez, G. (2004). Statistical criteria to establish bioassay programs. *Health Phys.* (to appear)
- [4] López-Fidalgo and Rodríguez-Díaz (2004). Elfving method for computing c-optimal designs in more than two dimensions *Metrika* (to appear)
- [5] Müller W.G. and Stehlík M. (2004). An example of D -optimal designs in the case of correlated errors. *COMPSTAT'2004 Symposium*, Physica-Verlag: New York.
- [6] Sánchez, G. (2004). Statistical Criteria To Estimate The Internal Doses In Workers Exposed To Radioactive Airbornes. *IRPA 11 Proceedings ???*
- [7] Sánchez, G. and López-Fidalgo, J. (2003). Mathematical techniques for solving analytically large compartmental systems. *Health Phys.* 85(2), 184-193, 2003.

- [8] Skrable K.W. (1974). A general equation for the kinetics of linear first order phenomena and suggested applications. *Health Phys.* 27, 155-157.

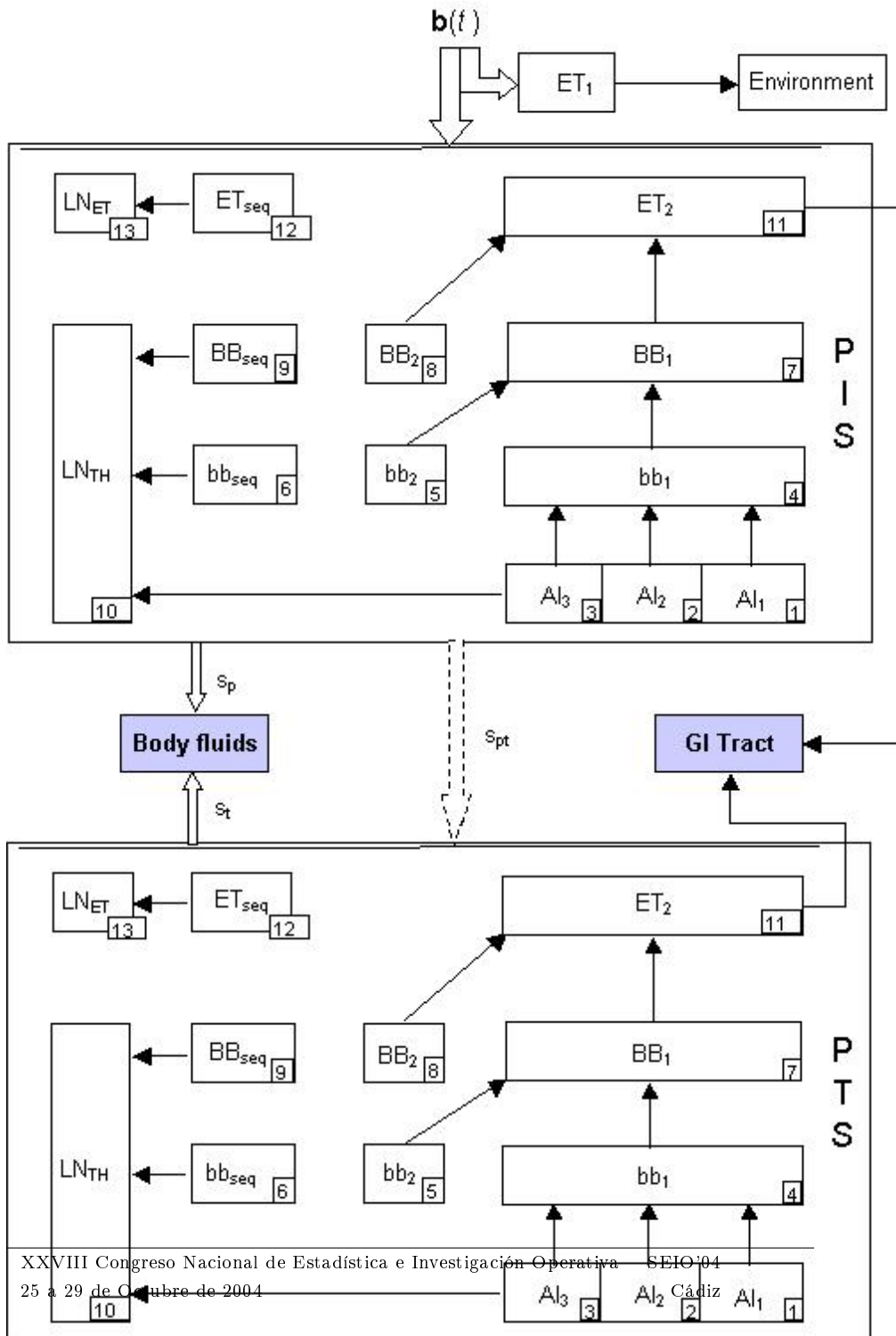
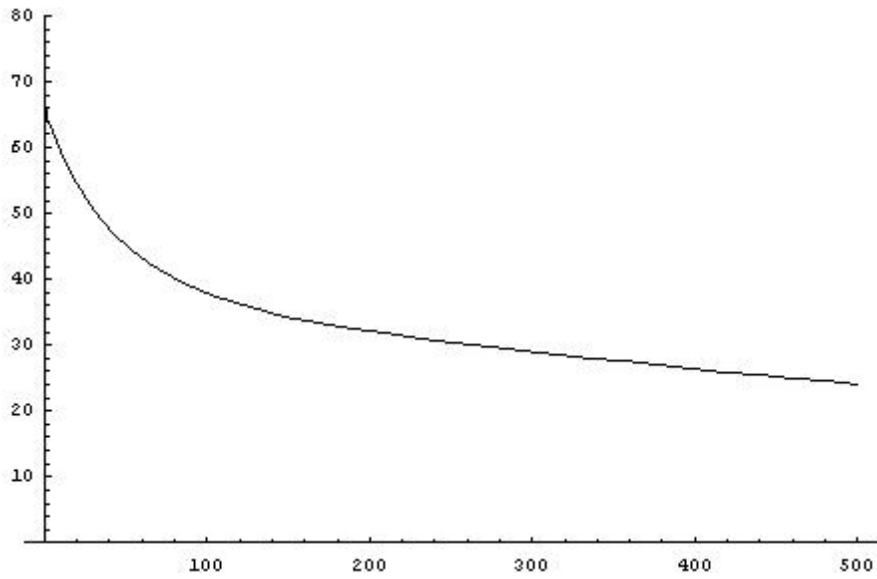
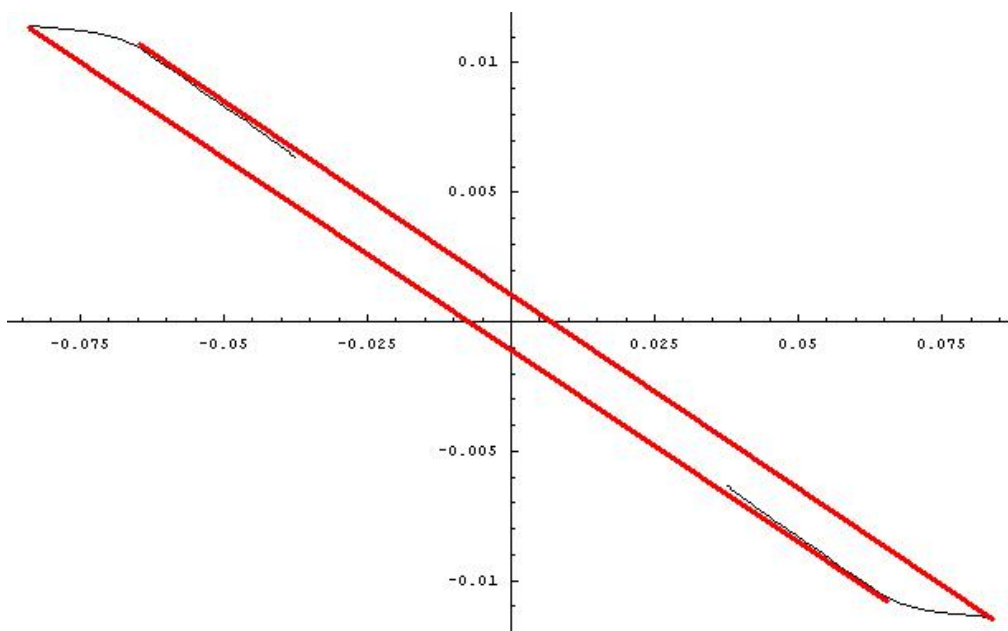


Figure 2: ICRP 66 Respiratory Tract Model. The dashed arrow from subsystem PIS to subsystem PTS means that the flow goes from each compartment in PIS to the compartment with the same number in PTS. The hollow arrow \Rightarrow means a flow from each compartment in subsystem PIS or PTS to the “Body fluid”. A simple arrow \rightarrow means flow from a single compartment to another.

Figure 3: Original model, for $I=1000$, $p=5$ Figure 4: Elfving's set for $I=1000$, $p=5$

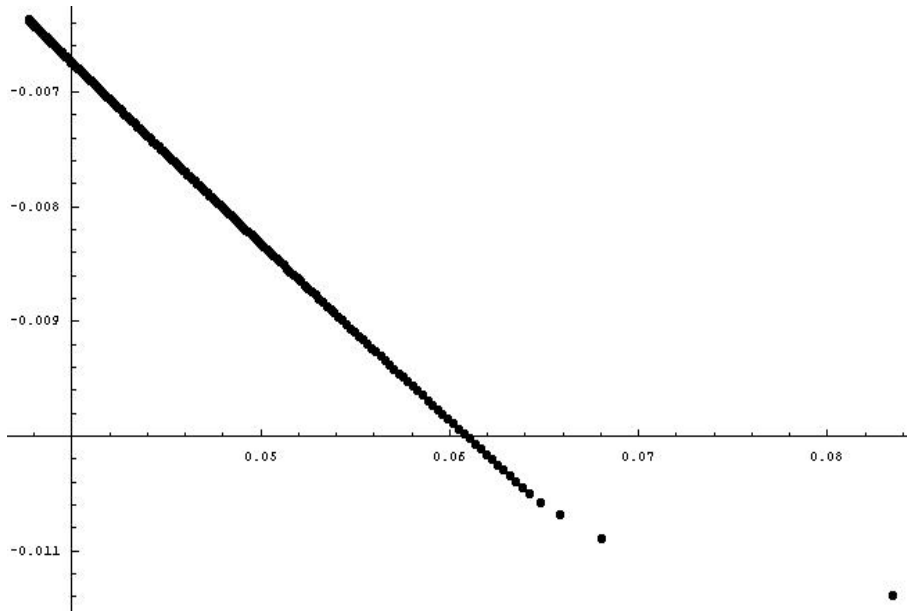


Figure 5: Curvature of the linearized model. Elfving's loci for $\Delta t = 0.5$

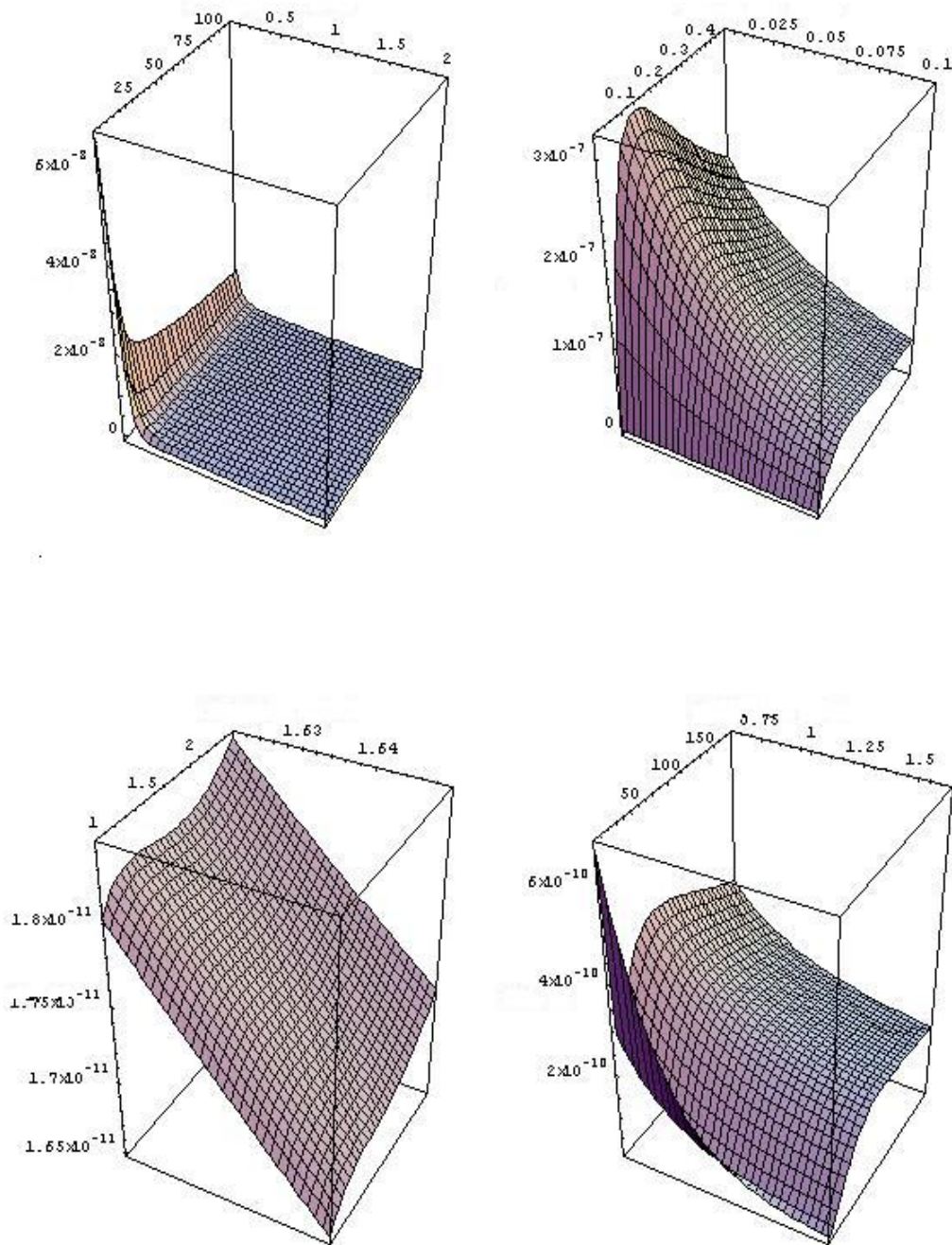


Figure 6: $\text{Det}(M)$ for different designs $\xi = \{t_1, t_1 + d\}$ (Original Model)